crystals

MDPI

Article

Electronic Heat Capacity and Lattice Softening of Partially Deuterated Compounds of κ-(BEDT-TTF)$_2$Cu[N(CN)$_2$]Br

Yuki Matsumura [1], Shusaku Imajo [2], Satoshi Yamashita [1], Hiroki Akutsu [1] and Yasuhiro Nakazawa [1,*]

[1] Department of Chemistry, Graduate School of Science, Osaka University, Machikaneyama 1-1, Toyonaka, Osaka 560-0043, Japan; matsumuray16@chem.sci.osaka-u.ac.jp (Y.M.); sayamash@chem.sci.osaka-u.ac.jp (S.Y.); akutsu@chem.sci.osaka-u.ac.jp (H.A.)

[2] Institute for Solid State Physics, University of Tokyo, Kashiwa, Chiba 277-8581, Japan; imajo@issp.u-tokyo.ac.jp

* Correspondence: nakazawa@chem.sci.osaka-u.ac.jp

Abstract: Thermodynamic investigation by calorimetric measurements of the layered organic superconductors, κ-(BEDT-TTF)$_2$Cu[N(CN)$_2$]Br and its partially deuterated compounds of κ-(d[2,2]-BEDT-TTF)$_2$Cu[N(CN)$_2$]Br and κ-(d[3,3]-BEDT-TTF)$_2$Cu[N(CN)$_2$]Br, performed in a wide temperature range is reported. The latter two compounds were located near the metal–insulator boundary in the dimer-Mott phase diagram. From the comparison of the temperature dependences of their heat capacities, we indicated that lattice heat capacities of the partially deuterated compounds were larger than that of the pristine compound below about 40 K. This feature probably related to the lattice softening was discussed also by the sound velocity measurement, in which the dip-like structures of the $\Delta v/v$ were observed. We also discussed the variation of the electronic heat capacity under magnetic fields. From the heat capacity data at magnetic fields up to 6 T, we evaluated that the normal-state γ value of the partially deuterated compound, κ-(d[3,3]-BEDT-TTF)$_2$Cu[N(CN)$_2$]Br, was about 3.1 mJ K^{-2} mol^{-1}. Under the magnetic fields higher than 3.0 T, we observed that the magnetic-field insulating state was induced due to the instability of the mid-gap electronic state peculiar for the two-dimensional dimer-Mott system. Even though the volume fraction was much reduced, the heat capacity of κ-(d[3,3]-BEDT-TTF)$_2$Cu[N(CN)$_2$]Br showed a small hump structure probably related to the strong coupling feature of the superconductivity near the boundary.

Keywords: organic superconductor; strong electron correlations; heat capacity; Mott transition

check for updates

Citation: Matsumura, Y.; Imajo, S.; Yamashita, S.; Akutsu, H.; Nakazawa, Y. Electronic Heat Capacity and Lattice Softening of Partially Deuterated Compounds of κ-(BEDT-TTF)$_2$Cu[N(CN)$_2$]Br. *Crystals* **2022**, *12*, 2. https://doi.org/10.3390/cryst12010002

Academic Editor: Andrei Vladimirovich Shevelkov

Received: 6 November 2021
Accepted: 19 December 2021
Published: 21 December 2021

Publisher's Note: MDPI stays neutral with regard to jurisdictional claims in published maps and institutional affiliations.

Copyright: © 2021 by the authors. Licensee MDPI, Basel, Switzerland. This article is an open access article distributed under the terms and conditions of the Creative Commons Attribution (CC BY) license (https://creativecommons.org/licenses/by/4.0/).

1. Introduction

It is generally recognized that strong electron correlations in the half-filling state tend to induce a metal–insulator transition, which is called the Mott transition [1–3]. Unusual electronic phenomena such as high-T_c superconductivity [4,5], anomalous mass enhancement of electron carriers [6,7], non-Fermi liquid features [8], and charge disproportionation [9], are known to emerge around the transition. These phenomena are dominated by the Mott–Hubbard physics, which describes the competitive nature of the itinerancy and localization of correlated electrons. The two-dimensional (2D) organic charge transfer compounds with the chemical formula of κ-(BEDT-TTF)$_2$X, where BEDT-TTF is bis(ethylenedithio)tetrathiafulvalene and X is the monovalent counter anion, are known as a typical electron correlation system of π-electrons originating from molecular HOMOs. These compounds give a phase relation determined by the ratio of the on-site or inter-site Coulomb repulsion U, V, and bandwidth W, which is tunable by pressure. Their physical properties are summarized as a so-called 2D dimer-Mott-type phase diagram, where the antiferromagnetic insulating phase and the metallic/superconductive phase are adjacent to each other [10,11]. The insulating phase and the superconductive phase are separated by the first-order Mott boundary. The existence of the critical endpoint at a finite temperature and the rounding of the Mott transition line [12] as well as the disorder-sensitive electronic

states due to the glassy feature of ethylene groups make the curious merging of the electronic and phonon states near the boundary [13]. Furthermore, the peculiar criticality across the first-order boundary [14,15] and the unusual softening of lattice dynamics, known as critical elasticity, are now being discussed by the sound velocity and the thermal expansion measurements [16–18].

To further investigate the unusual features in physical properties just near the boundary in terms of multiple degrees of freedom, such as spin, charge, and lattice, information on thermodynamic properties is important. However, the experiments under pressure can detect only the relative change of thermal anomalies with the standard calorimetric technique under external pressures. Pursuing the systematic change of thermodynamic parameters from the accurate values of the heat capacity just near the boundary region is required for this purpose. The partial deuteration of donors [19–21] or solid solutions of halogen sites in the counter anions of $Cu[N(CN)_2]X$ (X = Br and Cl) [22,23] are performed for the purpose of chemical-pressure tuning to approach the critical boundary from the position of bulk superconductor, κ-$(BEDT\text{-}TTF)_2Cu[N(CN)]_2]Br$ in the phase diagram. According to the results by Kawamoto et al., single crystals synthesized by the BEDT-TTF molecule, of which ethylene groups on both sides are partially deuterated, can tune chemical pressure systematically [19]. They labeled the deuterated ratio with the notation of d[*n*,*n*] to represent the number of the deuterium in each ethylene group. The increase of the substitution rate can change the position of the compound with the $Cu[N(CN)_2]Br^-$ anion to the Mott boundary gradually. κ-(d[0,0]-BEDT-TTF)$_2$Cu[N(CN)]$_2$]Br (d[0,0] compound, hereafter) shows bulk superconductivity below 11–12 K, while fully deuterated κ-(d[4,4]-BEDT-TTF)$_2$Cu[N(CN)]$_2$]Br (d[4,4] compound) located in the Mott-insulating region undergoes an antiferromagnetic transition around 15 K. According to the transport measurements, the compound with d[3,3]-BEDT-TTF (d[3,3] compound) is located very close to the boundary as is schematically illustrated in Figure 1 [19,24]. Using the partially deuterated d[2,2] and d[3,3] compounds, thermodynamic information related to the electronic and the lattice states just near the boundary are possible to be detected through the single-crystal calorimetry technique and sound velocity measurements.

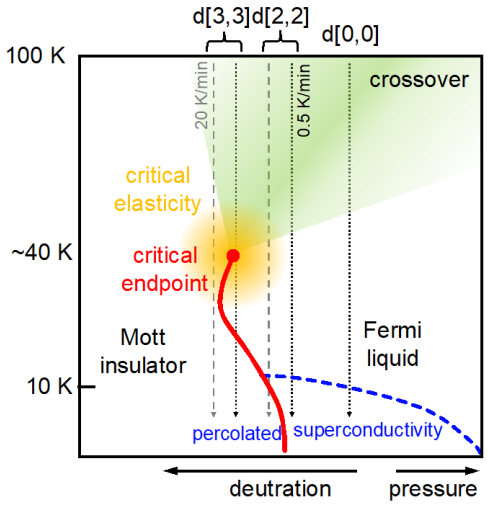


Figure 1. A schematic view of the two-dimensional (2D) dimer-Mott phase diagram for the κ-$(BEDT\text{-}TTF)_2X$ system. The positions of the d[0,0], d[2,2], and d[3,3] compounds in a slowly cooled case are shown by the dashed arrows. The possible positions for the rapidly cooled cases (20 K min^{-1}) for the latter two compounds are also shown by the gray dashed arrows. The position of the Mott boundary and that of the critical endpoint are shown in the red color.

2. Experiments

Low-temperature heat capacity measurements were performed by the thermal relaxation calorimeters designed for measuring single-crystal samples and pellet samples of

molecule-based compounds. The plate-like single crystals of the d[2,2] and d[3,3] compounds weighing 2–3 mg were attached to the sample stage by a small amount of Apiezon N grease for low-temperature measurements with magnetic fields applied perpendicularly to the conducting plane. A ruthenium oxide sensor of which the resistance at room temperature is 10 kΩ was used for the sample-temperature sensor in the low-temperature experiments between 0.7 K and 3 K, and a Cernox1070 bare chip sensor (LakeShore, Westerville, OH, USA) was used for the experiments between 5 K and 100 K. The details of the relaxation calorimetry systems including measurements under magnetic fields are reported in the literature [25]. The higher-temperature heat capacity of the d[0,0] compound was measured by a adiabatic calorimeter using multiple pieces weighing about 25 mg. The thermometer for the adiabatic calorimetry cell was a Pt chip sensor which was calibrated between 20 K and 300 K. The accuracy of the thermal relaxation technique is within a few percentages of the absolute values, and the relative precision was about 0.5% for the present measurements. The sound velocity measurements were performed for block-type single-crystal samples of the d[2,2] and d[3,3] salts. The change of the sound velocities transmitted in the crystal was measured by the longitudinal ultrasound waves, of which the frequency was 30.5 MHz. They were generated and detected by $LiNbO_3$ piezoelectric transducers (thickness: 100 μm) attached to the side surfaces of the crystals of which details were similar to those in reference [26]. We applied ultrasonic sounds so as to propagate in the in-plane direction which was sensitive to the electronic states.

3. Results and Discussion

In Figure 2a, we show the temperature dependences of the heat capacity of the d[0,0] and d[3,3] compounds in a logarithmic plot. The red color represents the data of the d[0,0] compound from 0.8 K to 288 K. The low-temperature data below 20 K were obtained by the thermal relaxation technique as was already reported in references [27,28], and the higher temperature data were obtained by an adiabatic calorimeter. The black curve shown in the temperature range below 20 K is the normal state heat capacity obtained by fitting the data with 8 T, which was applied perpendicular to the conducting layer. The low-temperature data have already been reported by several groups [29–32].

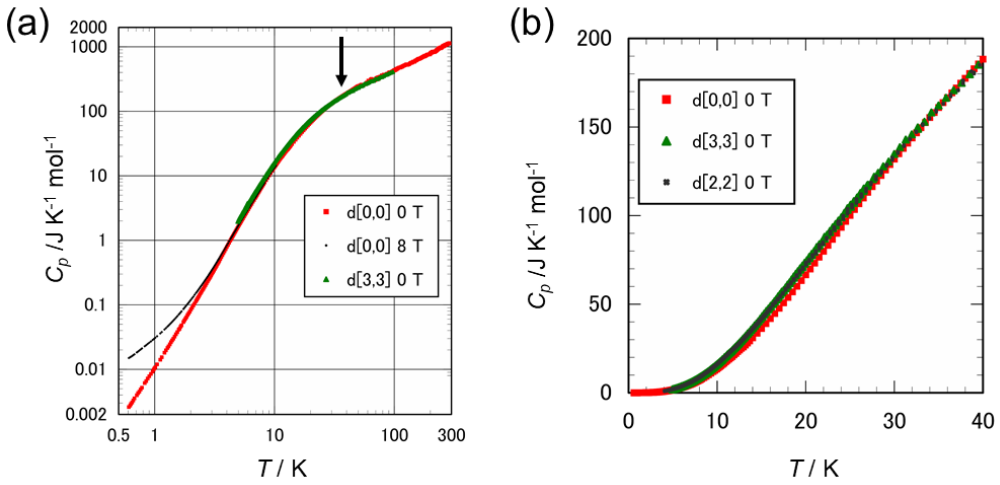


Figure 2. (**a**) Temperature dependences of the heat capacity of κ-(BEDT-TTF)$_2$Cu[N(CN)$_2$]Br (d[0,0] compound) shown by red squares and its partially deuterated compound (d[3,3] compound) denoted by green triangles shown in a logarithmic plot. The black dots show the data for the normal state heat capacity determined from the data in reference [27]. The arrow indicates the temperature of the critical endpoint of the Mott boundary. (**b**) C_p vs. T lot of the d[0,0], d[2,2], and d[3,3] compounds in a temperature range below 40 K, which shows the difference of the lattice heat capacity between the partially deuterated compound and the pristine compound.

From the overall temperature dependence of the d[0,0] compound, the phonon structure of the κ-type BEDT-TTF salts showed a Debye-like temperature dependence in the low-temperature region due to acoustic phonons. It showed a further increase above 100 K due to the multiple optical phonon modes and molecular vibrations. This feature is similar to the cases of typical molecular crystals [33]. We also showed the heat capacity data of the d[3,3] compound obtained for a single crystal between 4.9 K and 100 K in Figure 2a. The measurement of this sample was performed by slow cooling conditions from room temperature down to 4 K with a rate lower than 0.1 K min^{-1}. Although the data are shown in the logarithmic plot in the figure, the difference of the green and red curves observed below about 40 K means that the lattice heat capacity of the partially deuterated salt became larger than the pristine non-deuterated d[0,0] compound. From the figure, it is noted that the difference appeared below the region of the critical endpoint temperature that is shown by the arrow in the figure. To confirm the difference of the heat capacity between the two compounds, we showed the data below 40 K in C_p vs. T plot in Figure 2b. The difference was about 10–15% of the absolute values around 20 K, which exceeded the possible error bars related to the accuracy of the present heat capacity measurement. This difference was not originated from the spin entropy, since the κ−(BEDT-TTF)$_2$Cu[N(CN)$_2$]Cl having the bulk antiferromagnetic ordering showed a smaller heat capacity in this temperature region as was reported in references [10,11]. The increase of the heat capacity in the partially deuteration can be confirmed also in the data of the d[2,2] compound shown in Figure 2b, which were measured in slow cooling conditions. The difference from the d[0,0] data was slightly smaller, but a similar behavior to that of the d[3,3] compound seemed to exist. Although we do not have direct evidence at present, we speculate that the phonon structure shows a glassy feature due to the rounding of the phase boundary and merging of the Mott-insulating phase and the metallic phase. The lattice softening that gives a higher density of states of phonons occurs in the compounds just near the boundary can be understood as a kind of supercritical phenomenon that specifically appears near the boundary. Divergent compressibility has been reported by thermal expansion measurements [17,18,34].

The peculiar softening of the acoustic phonons of the partially deuterated d[2,2] and d[3,3] compounds below about 40 K, similar to the reported softening in κ-(BEDT-TTF)$_2$Cu[N(CN)$_2$]Cl [16] under pressures, was detected by the sound velocity measurement. The datasets shown in Figure 3 were the relative change in the ultrasonic sound velocity $\Delta v/v$ of the d[2,2] and d[3,3] compounds between 5 K and 100 K obtained for the cases with different cooling rates of 0.5 K min^{-1} and 20 K min^{-1}. $\Delta v/v$ showed a peculiar dip structure, indicating a tendency of significant lattice softening in a temperature range between 20 K and 50 K, and the temperatures showing the minima were 34 K for 20 K min^{-1} and 38 K for 0.5 K min^{-1} for the d[3,3] compound. Here, we emphasize that the temperature region where the decrease of the sound velocity took place was roughly corresponding to the region where the larger heat capacity appeared.

This fact demonstrated that these phenomena originated from the same origin. Although it is still a speculative discussion, the softening response of the ultrasonic compressional wave at this region implied that the coherence of acoustic phonons was disturbed by the microscopic merging of electronic phases and gave a kind of glassy state in a microscopic level. The observed experimental results are consistent with the experiment of κ-(BEDT-TTF)$_2$Cu[N(CN)$_2$]Cl with gas pressure control [16]. Indeed, although the accurate estimation of the absolute value of the ultrasonic attenuation is difficult owing to the significant lattice softening, the enhancement of the attenuation, which implies the growth of the phonon scattering, was observed in this region. By comparing the sound velocity data of the d[2,2] compound with those of the d[3,3] compound, we can find that the position of the dip structures shifted to a higher temperature and became much broader, since d[2,2] was located in the metallic region. The broadening of the hump agreed with the change in the position in the phase diagram. The shifts of the dip temperature by changing the cooling rate in both compounds should be related to the change of the positions of the d[2,2] and d[3,3] compounds in the phase diagram. As is known for this compound, the disorder

in ethylene groups of BEDT-TTF molecules induced by rapid cooling made the volume large. The rapid cooling worked as a negative pressure effect. We roughly evaluated the possible positions of each cooling rate and displayed them in the phase diagram in Figure 1. The phonon softening near the boundary region is probably consistent with the unusual elasticity near the boundary reported by thermal expansion measurements [17,18]. It is important to measure the frequency dependences of $\Delta v/v$ in order to evaluate the glassy feature of the phonons. However, higher frequency measurements were not easy because of the strong reduction in the signals of ultrasonic echoes. The crossing of the 1st-order Mott boundary at low temperatures can also give an anomaly in sound velocity. Although we cannot see drastic discontinuity in $\Delta v/v$ at present, the small kink around 25 K observed in the slowly cooled d[3,3] salt (light blue) may be attributed to the 1st-order Mott transition, which was typically less significant than the critical elasticity around the critical endpoint as reported in reference [16].

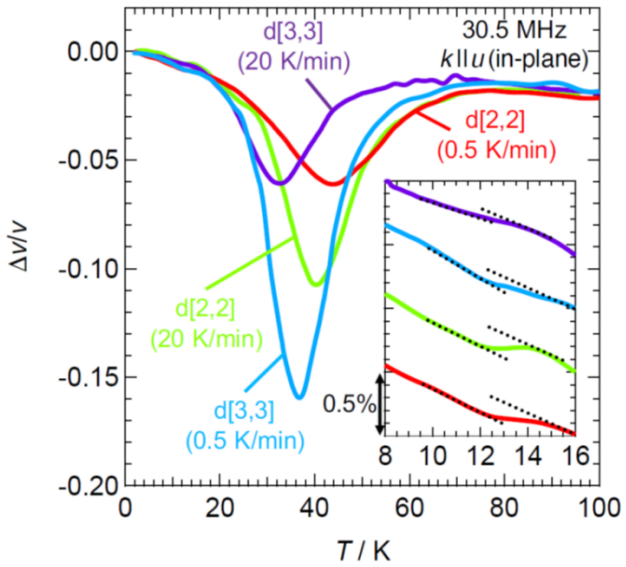


Figure 3. Temperature dependences of the relative change of the sound velocity ($\Delta v/v$) for the partially deuterated d[3,3] compound and d[2,2] compound obtained with two cooling rates of 0.5 K min^{-1} and 20 K min^{-1}. The inset shows the sound velocity anomaly around the superconducting transition temperature.

The inset of Figure 3 shows the sound velocity anomalies around the superconducting transition temperature of the d[3,3] and d[2,2] compounds. The sound velocity was sensitive to detect the superconductivity including the fluctuating superconductivity. Since the fluctuations of the superconductivity also made the lattice softened, the change in the sound velocity tended to occur at higher temperatures than T_c of the bulk superconductivity. The onset and the local minimum around 11–13 K of the dip typically correspond to the emergence of the fluctuating superconductivity and the superconducting transition, respectively. The present experiments were performed in the configuration in which ultrasonic sounds propagated in the in-plane direction. The absolute value of the change seemed to be larger than those in the previous measurements of interlayer ultrasonic responses for the d[0,0] compound [35] and κ-(BEDT-TTF)$_2$Cu(NCS)$_2$ [36], despite the percolative superconductivity originated from the macroscopic phase separation near the Mott transition in the present d[2,2] and d[3,3] compounds. The magnitude of the dip in the inset demonstrated that the volume fraction of the superconducting components changed due to the difference of deuterated numbers and cooling rates. This sensitive acoustic response to the superconductivity enabled us to discuss the details of the superconductivity including the fluctuating superconductivity and percolative superconductivity. In addition, it suggests a possibility to detect other superconducting state such as the Fulde–Ferrell–Larkin–Ovchinnikov (FFLO)

superconductivity in the d[0,0] compound and other organic superconductors [37–40]. As a matter of fact, the FFLO state in the κ-(BEDT-TTF)$_2$Cu[N(CN)$_2$]Br was detected in the high-field ultrasound measurement by Imajo et al. [38].

The electronic properties related to the percolative feature of the superconductive and antiferromagnetic components near the boundary can be discussed through the analyses of the magnetic fields dependences of electronic heat capacity coefficient γ and lattice heat capacity coefficient β of the d[3,3] compound. It is known that the volume fraction of the superconductivity of this compound was significantly suppressed and the number of electrons related to the superconducting components became smaller than that of the d[0,0] compound.

In Figure 4a,b, we show the heat capacity data at extremely low temperatures between 0.7 K and 2.64 K (T^2 = 7 K^2) measured in magnetic fields up to 6 T. The data were plotted in C_pT^{-1} vs. T^2. Here, the magnetic fields were applied perpendicularly to the superconducting layers. From the heat capacities at 0 T, 0.5 T, 1 T, and 1.5 T in Figure 4a, we can notice that the C_pT^{-1} showed almost a linear dependence against T^2 in this low-energy region. The γ and the β for each magnetic field were determined using a linear fit $C_pT^{-1} = \gamma + \beta T^2$ to the data below 2 K. In Table 1, we show the two thermodynamic parameters γ and β obtained by the fitting analysis. The γ value at 0 T was about 1.3 ± 0.2 mJ K^{-2} mol^{-1}, reflecting on the gap formation in the superconductive ground state. A slight increase of γ in a low-filed region below 1.0 T indicated the gradual recovery of the electron density of states induced by the application of magnetic fields, although the values of γ were still very small. In fact, when applying magnetic fields with an out-of-plane configuration for various layered superconducting compounds, the pair-breaking mainly due to the orbital effect induced normal electrons. In the bulk superconductor of the d[0,0] compound, the recovery rate of the C_pT^{-1} obeyed the square root of H, which was discussed as an evidence of the nodal superconductor explained by Volovik's theory. The d[0,0] compound showed a typical feature of the d-wave symmetry from the angle-resolved heat capacity measurements [27,28], and the normal state γ was evaluated as 22–25 mJ K^{-2} mol^{-1}. The pair-breaking feature was also reported in the d[1,1] and d[2,2] compounds in reference [41]. However, the change in γ by external magnetic fields was reported as negligibly small for the d[4,4] compound and κ-(BEDT-TTF)$_2$Cu[N(CN)$_2$]Cl located in the insulating region [41]. Although much smaller than d[2,2], the increase of the γ term observed below 1.0 T for d[3,3] demonstrated that the normal-state γ value detected was considered as ~3.1 mJ K^{-2} mol^{-1}.

Table 1. The thermodynamic parameters of the electronic heat capacity coefficient, γ, and the Debye term, β, for each magnetic field between 0 T and 6 T.

μ0 (H/T)	B (mJ K^{-4} mol^{-1})	Γ (mJ K^{-2} mol^{-1})
0	12.5	1.3
0.5	12.0	2.2
1	12.0	3.1
1.5	12.2	2.9
3.5	12.9	2.0
4	13.1	1.9
4.5	13.6	1.6
6	13.1	0.9

The heat capacity data obtained at higher magnetic fields of 3.5 T, 4.0 T, 4.5 T, and 6 T are shown in Figure 4 b. A curious tendency different from the pair breaking appeared in the temperature dependence of the electronic heat capacity. The C_pT^{-1} vs. T^2 plots of 3.5 T, 4.0 T, and 4.5 T showed small hump-like structures around T = 1.4–1.7 K, and they were suppressed in the higher magnetic field of 6 T. The feature was different from the contribution of simple paramagnetic spins, which should give a Schottky-like heat capacity, since the Schottky anomaly gives the systematic change due to the increase of Zeeman splitting. The γ values in these fields were smaller than those of the data at H = 1.5 T. It

is emphasized that the data at H = 6 T gave a much smaller γ value of 0.9 mJ K^{-2} mol^{-1}, which is a comparable value with that at H = 0 T.

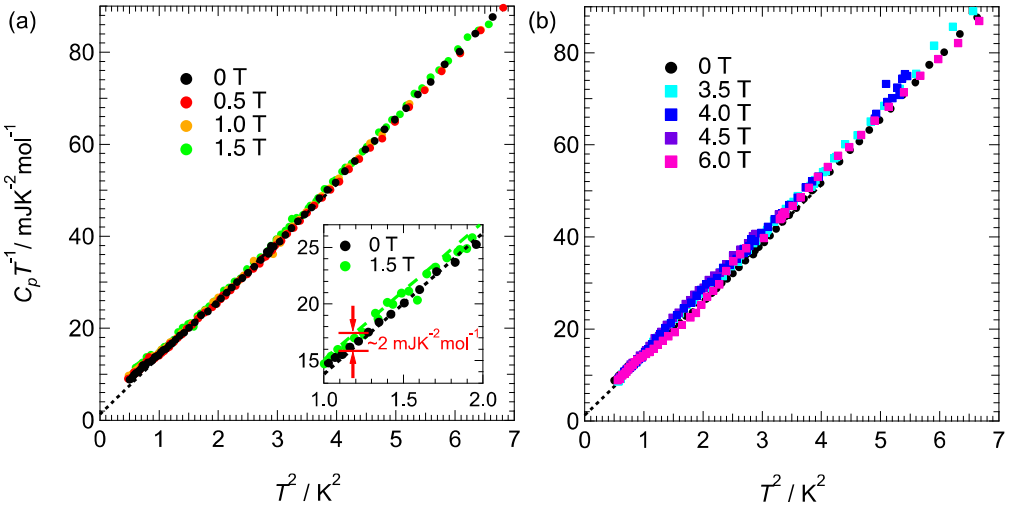


Figure 4. C_pT^{-1} vs. T^2 plot of the partially deuterated d[3,3] compound obtained under magnetic fields applied perpendicular to the donor layer. The lower-field data of 0 T, 0.5 T, 1.0 T, and 1.5 T are shown in (**a**), and those at higher fields of 3.5 T, 4.0 T, 4.5 T, and 6.0 T are shown in (**b**) together with the data at the magnetic field of 0 T. The broken line represents the fitting result of 0 T using $C_pT^{-1} = \gamma + \beta T^2$. The inset in (**a**) is an enlarged plot of the datasets at magnetic fields of 0 T and 1.5 T around 1.0 K to make the field dependence clearer.

Figure 5 displays the change in these parameters in magnetic fields. It was confirmed that β was 12.5 $\pm$ 0.1 mJ K^{-4} mol^{-1} at 0 T, which is almost consistent with the previous report of κ-(BEDT-TTF)$_2$Cu[N(CN)$_2$]Br, and the change in β with the increase of the magnetic field was relatively small, as is shown in the figure. The change in the γ value with the magnetic field showed unusual features as the superconductive materials. From the variation of γ in the higher-field region, we should note that the shift of the Mott boundary, as was suggested by the transport measurements by Taniguchi et al., certainly occurs in this compound at this boundary region [24,42]. The normal state γ was evaluated by using the value at the peak in Figure 5 as 3.1 mJ K^{-2} mol^{-1}, although it must be an underestimate due to the field-dependent Mott boundary.

The change in the thermodynamic parameter γ inside the superconducting region in the dimer-Mott phase diagram was discussed from the theoretical and experimental viewpoints. According to the previous study of the low-temperature heat capacity of partial deuterated salts with Cu[N(CN)$_2$]Br, the normal state γ term is evaluated as 20 mJ K^{-2} mol^{-1} for the d[1,1] compound and 9–10 mJ K^{-2} mol^{-1} for the d[2,2] compound. The d[4,4] compound is located in the insulating region, and its γ value reaches almost zero [43]. The d[3,3] compound measured in this work revealed that the normal state γ value was 3.1 mJ K^{-2} mol^{-1}, although the insulating phase partially merged by applying magnetic fields and the gap-like structure seemed to be enhanced under magnetic fields. The systematic decrease of γ that occurs when approaching the boundary is understood by the enhancement of the Hubbard-like picture due to the increase of the U/W ratio [44,45]. This feature is interpreted by a theoretical suggestion for strongly correlated electron systems given by Kotliar et al. using the dynamical mean-field approach, as is shown in Figure 6 [46]. The superconducting component in the d[3,3] samples may be formed in the situation where the band-like and Mott–Hubbard features coexist, mainly produced by the electrons in the mid-gap states. The delicate balance of the magnetic insulating state and the superconductivity may induce the curious magnetic field dependence in the low-temperature thermal excitations for this material. It is considered that the bulk superconducting compounds, such as κ-(BEDT-TTF)$_2$I$_3$, κ-(BEDT-TTF)$_2$Ag(CN)$_2$H$_2$O, κ-

$(BEDT\text{-}TTF)_2Cu(NCS)_2$, are in the Fermi liquid region and the Brinkman–Rice enhancement emerges as was reported previously [47]. The crossover from the Brinkmann–Rice region to the Hubbard-gap region is considered as a specific feature of the 2D dime-Mott compound. Such a crossover can be explained by the picture schematically illustrated in Figure 6. The unconventional nature of the superconductivity was characterized by the four-fold oscillation of C_pT^{-1} in the angle-resolved heat capacity measurements, which demonstrated that the antiferromagnetic spin fluctuations play an important role for relatively high transition temperatures of the dimer-Mott superconductors. The symmetry change of Cooper pairs from d_{xy} for κ-$(BEDT\text{-}TTF)_2Ag(CN)_2H_2O$ to $d_{x2-y2} + s_{\pm}$ for the d[0,0] compound occurs inside the superconductive phase [28,48–53]. The relation with the symmetry change and the crossover inside the superconducting phase are interesting subjects to be solved by heat capacity measurements, although it is still a speculative discussion at present.

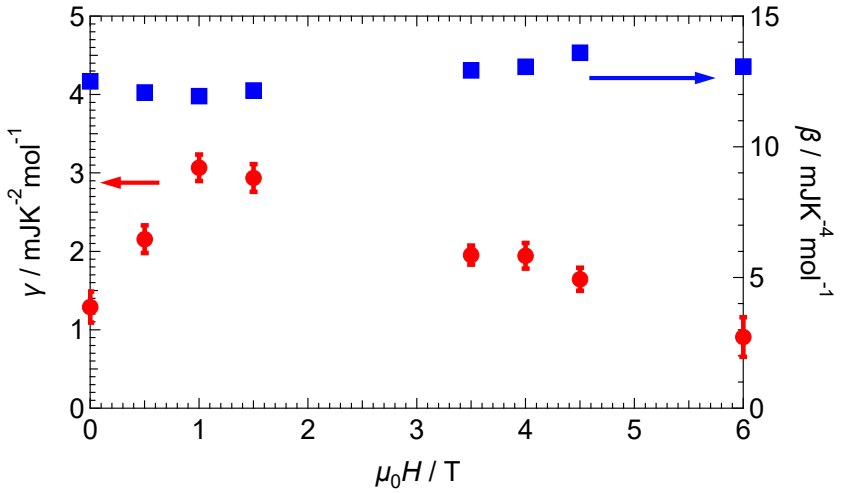


Figure 5. Magnetic fields dependence of the thermodynamic parameters γ and β of the d[3,3] compound. The peak structure at 1.0 T means that the normal state electronic heat capacity coefficient of this compound was about 3.0 mJ K^{-2} mol^{-1}. The decrease of γ above this field means that an insulating component was induced in the high-field region. The translucent curves are guides for the eye.

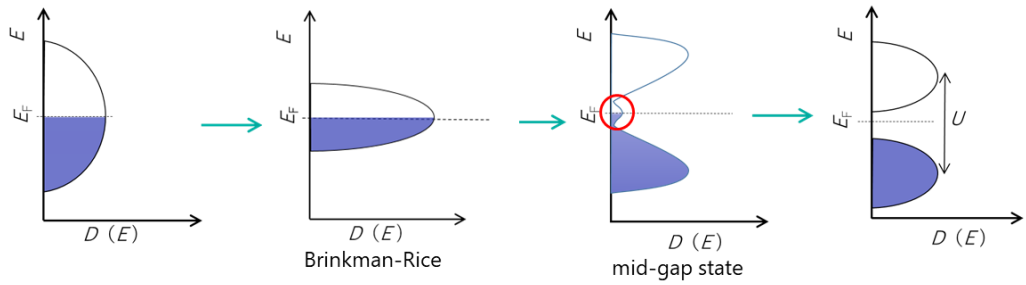


Figure 6. Schematic illustration of the electronic structure expected for the dimer-Mott compounds. Normal band metal on the left side gradually changed to the Mott–Hubbard state with the increase of U/W ratio. The variation from the Brinkman–Rice region to the mid-gap state region may be realized with the increase of partially deuteration.

Finally, we discussed the heat capacity jump, ΔC_p, around the superconductive transition of the d[3,3] compound. The non-deuterated d[0,0] compound showed a large heat capacity jump with about ΔC_pT^{-1} of 60 mJ K^{-2} mol^{-1}, and this anomaly was suppressed by applying magnetic fields above H_{c2}. The data of the d[0,0] compound showing the thermal anomaly are shown in Figure 7a. These results were already reported in references [27,28]. The temperature dependence of C_pT^{-1} of the d[3,3] compound is shown in

the green color in the same figure. The absolute value of C_pT^{-1} was 15% larger than that of d[0,0] at 10 K due to the difference in the lattice heat capacity as mentioned above. The heat capacity jump around T_c of the d[3,3] compound was quite small as compared with that of the d[0,0] compound but visible as a broad hump in the temperature dependence plot of C_pT^{-1} in Figure 7b. The suppression of this hump by the application of a magnetic field of 6 T indicated that the superconducting component certainly existed. The ΔC_pT^{-1} was roughly evaluated at most as 10 mJ K^{-2} mol^{-1} and the transition temperature was about 11 K, although the large lattice heat capacity gave ambiguity for the accurate determination of these electronic components. Since this compound was located just near the boundary, the much-reduced value of ΔC_pT^{-1} was of course consistent with the smaller normal state γ value. In spite of the smaller fraction in the d[3,3] compound, the large value of $\Delta C_p/\gamma T$~3.2 indicated that the strong coupling feature of the superconductivity was retained. Here, we assumed the peak value of γ in Figure 5 was close to the normal state γ value. It may be underestimated, if we considered the relatively smaller magnetic field of 1T was used for the evaluation of the normal-state γ value. However, the tendency of the enhanced electron correlations near the boundary gives a strong attractive force for electron pairs [44], although the diminishing of electrons which contribute to the density of states in the mid-gap state is serious for stabilizing bulk superconductivity.

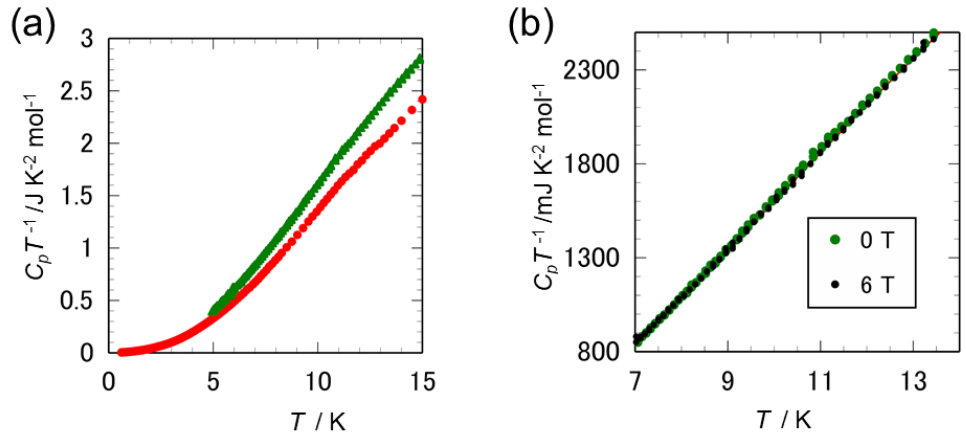


Figure 7. (**a**) C_pT^{-1} vs. T plot of the heat capacity of the d[0,0] compound (red color) and that of the d[3,3] compound (green color) obtained at 0 T; (**b**) the extended plot around the superconducting transition of the d[3,3] compound obtained at 0 T and 6 T. The data at magnetic fields of 0 T and 6 T are shown by the green circles and the black circles, respectively. A broad and small hump around the transition seemed to be suppressed by an external magnetic field.

4. Summary

The thermodynamic properties of κ-(BEDT-TTF)$_2$Cu[N(CN)$_2$]Br and partially deuterated d[3,3] compound have been studied by the heat capacity measurements with the thermal relaxation and the adiabatic calorimetry techniques. The d[3,3] compound located just near the boundary showed a larger heat capacity than the pristine compound at low temperatures below 40 K. This feature was confirmed by the sound velocity measurement as the significant lattice softening originating from the critical elasticity. The low-temperature heat capacity in magnetic fields demonstrated that the normal-state γ value was about 3.1 mJ K^{-2} mol^{-1}. The magnetic fields higher than 3.0 T were found to induce a gapped insulating state, and this field-induced feature was interpreted in terms of the instability of the mid-gap state that occurred due to the enhanced electronic correlations around the Mott boundary. Although the volume fraction was much reduced in the d[3,3] compound, the heat capacity data showed a small hump structure probably related to the strong-coupling feature of the superconductivity just near the boundary. This feature was also considered as the result of the larger U/W ratio near the boundary.

Author Contributions: Y.M., S.I. and S.Y. conducted the low-temperature heat capacity measurements. H.A. and Y.M. worked on sample characterization. The sound velocity measurements were performed by S.I., Y.M. and Y.N. designed the research plan, and all authors worked on the overall discussions throughout the work. Y.M. and Y.N. wrote the draft of the manuscript, and all authors commented on the manuscript. All authors have read and agreed to the published version of the manuscript.

Funding: This research was financially supported by JSPS KAKENHI (grant numbers: JP19K221690 and JP20H018620).

Institutional Review Board Statement: Not applicable.

Informed Consent Statement: Not applicable.

Data Availability Statement: The data presented in this study are available on request from the corresponding author.

Acknowledgments: The authors thank A. Kawamoto (Hokkaido University) and Hiromi Taniguchi (Saitama University) for valuable discussion in terms of crystal synthesis and sample characterization. Y.M. thanks JSPS for the fellowship for young researchers.

Conflicts of Interest: The authors declare no conflict of interest.

References

1. Mott, F.N. The transition to the metallic state. *Plilos. Mag.* **1961**, *6*, 287–309. [CrossRef]
2. Mcwhan, B.D.; Rice, M.T.; Tokura, Y. Metal-insulator transition in Cr-Doped V_2O_3. *Phys. Rev. Lett.* **1969**, *23*, 1384–1387. [CrossRef]
3. Imada, M.; Fujimori, A.; Tokura, Y. Metal-insulator transitions. *Rev. Mod. Phys.* **1998**, *70*, 1039–1263. [CrossRef]
4. Bednorz, J.G.; Müller, K.A. Possible high T_C superconductivity in the Ba-La-Cu-O System. *Z. Phys. B—Condens. Matter* **1986**, *64*, 189–193. [CrossRef]
5. Lee, A.P.; Nagaosa, N.; Wen, X.-G. Doping a Mott insulator: Physics of high temperature superconductivity. *Rev. Mod. Phys.* **2006**, *78*, 17–85. [CrossRef]
6. Stewart, R.G. Heavy-Fermion systems. *Rev. Mod. Phys.* **1984**, *56*, 755–787. [CrossRef]
7. Carter, A.S.; Rosenbaum, F.T.; Metcalf, P.; Honig, M.J.; Spalek, J. Mass enhancement and magnetic order at the Mott-Hubbard transition. *Phys. Rev. B* **1993**, *48*, 16841–16844. [CrossRef] [PubMed]
8. Von Löhneysen, H. Non-Fermi-liquid behaviour in the heavy-fermion system $CeCu_{6-x}Au_x$. *J. Phys. Condens. Matter* **1996**, *8*, 9689–9706. [CrossRef]
9. Hiraki, K.; Kanoda, K. Wigner Crystal Type of Charge Ordering in an Organic Conductor with a Quarter-Filled Band: $(DI-DCNQI)_2Ag$. *Phys. Rev. Lett.* **1998**, *80*, 4737–4740. [CrossRef]
10. Kanoda, K. Recent progress in NMR studies on organic conductors. *Hyperfine Interact.* **1997**, *104*, 235–249. [CrossRef]
11. Kanoda, K. Metal–Insulator Transition in κ-$(ET)_2X$ and $(DCNQI)_2M$: Two Contrasting Manifestation of Electron Correlation. *J. Phys. Soc. Jpn.* **2006**, *75*, 051007. [CrossRef]
12. Kagawa, F.; Miyagawa, F.; Kanoda, K. Magnetic Mott criticality in a κ-type organic salt probed by NMR. *Nat. Phys.* **2005**, *5*, 880–884. [CrossRef]
13. Akutsu, H.; Saito, K.; Sorai, M. Phase Behavior of Organic Superconductors, κ-$(BEDT\text{-}TTF)_2Cu[N(CN)_2]X$ (X = Br and Cl), Studied by ac Calorimetry. *Phys. Rev. B* **2000**, *61*, 4346–4352. [CrossRef]
14. Kagawa, F.; Miyagawa, K.; Kanoda, K. Unconventional critical behaviour in a quasi-two-dimensional organic conductor. *Nature* **2005**, *436*, 534–537. [CrossRef]
15. Sasaki, T.; Yoneyama, N.; Kobayashi, N. Mott transition and superconductivity in the strong correlated organic superconductor κ-$(BEDT\text{-}TTF)_2Cu[N(CN)_2]Br$. *Phys. Rev. B* **2008**, *77*, 054505. [CrossRef]
16. Fournier, D.; Poirier, M.; Castonguay, M.; Truong, D.K. Mott transition, Compressibility Divergence, and the *P-T* Phase Diagram of Layered Organic Superconductors: An Ultrasonic Investigation. *Phys. Rev. Lett.* **2003**, *90*, 127002. [CrossRef]
17. Gati, E.; Garst, M.; Manna, S.R.; Tutsch, U.; Bartosch, L.; Schubert, H.; Sasaki, T.; Sculueter, A.J.; Lang, M. Breakdown of Hookes law of elasticity at the Mott critical endpoint in an organic conductor. *Sci. Adv.* **2016**, *2*, e1601646. [CrossRef]
18. Gati, E.; Tutsch, U.; Naji, A.; Garst, M.; Köhler, S.; Schubert, H.; Sasaki, S.; Lang, M. Effects of Disorder on the Pressure-Induced Mott Transition in κ-$(BEDT\text{-}TTF)_2Cu[N(CN)_2]Cl$. *Crystals* **2018**, *8*, 38. [CrossRef]
19. Kawamoto, A.; Taniguchi, H.; Kanoda, K. Superconductor−Insulator Transition Controlled by Partial Deuteration in BEDT-TTF Salt. *J. Am. Chem. Soc.* **1998**, *120*, 10984–10985. [CrossRef]
20. Yoneyama, N.; Sasaki, T.; Kobayashi, N. Substitution Effect by Deuterated Donors on Superconductivity in κ-$(BEDT\text{-}TTF)_2Cu[N(CN)_2]Br$. *J. Phys. Soc. Jpn.* **2004**, *73*, 1434–1437. [CrossRef]
21. Müller, J.; Hartmann, B.; Sasaki, T. Fine-tuning the Mott metal–insulator transition and critical charge carrier dynamics in molecular conductors. *Philos. Mag.* **2017**, *97*, 3477–3494. [CrossRef]

22. Yasin, S.; Dumm, M.; Salameh, B.; Batail, P.; Meźière, C.; Dressel, M. Transport studies at the Mott transition of the two-dimensional organic metal κ-(BEDT-TTF)$_2$Cu[N(CN)$_2$]Br$_x$Cl$_{1-x}$. *Eur. Phys. J. B* **2011**, *79*, 383–390. [CrossRef]
23. Faltermeier, D.; Barz, J.; Dumm, M.; Dressel, M.; Drichko, N.; Petrov, B.; Semkin, V.; Vlasova, R.; Meźière, C.; Batail, P. Bandwidth-controlled Mott transition in κ−(BEDT−TTF)$_2$Cu[N(CN)$_2$]Br$_x$Cl$_{1-x}$: Optical studies of localized charge excitations. *Phys. Rev. B* **2007**, *76*, 165113. [CrossRef]
24. Taniguchi, H.; Kanoda, K.; Kawamoto, A. Field switching of superconductor-insulator bistability in artificially tuned organics. *Phys. Rev. B* **2003**, *67*, 014510. [CrossRef]
25. Sorai, M. *Comprehensive Handbook of Calorimetry and Thermal Analysis*; Wiley J. & Sons: West Susex, UK, 2004; pp. 68–74.
26. Imajo, S.; Akutsu, H.; Kurihara, R.; Yajima, T.; Kohama, Y.; Tokunaga, M.; Kindo, K.; Nakazawa, Y. Anisotropic Fully Gapped Superconductivity Possibly Mediated by Charge Fluctuations in a Nondimeric Organic Complex. *Phys. Rev. Lett.* **2020**, *125*, 177002. [CrossRef]
27. Imajo, S.; Yamashita, S.; Akutsu, H.; Nakazawa, Y. Quadratic temperature dependence of electronic heat capacities in the κ-type organic superconductors. *Int. J. Mod. Phys. B* **2016**, *30*, 1642014. [CrossRef]
28. Imajo, S.; Kindo, K.; Nakazawa, Y. Symmetry Change of d-wave Superconductivity in κ-type Organic Superconductors. *Phys. Rev. B* **2021**, *103*, L060508. [CrossRef]
29. Elsinger, H.; Wosnitza, J.; Wanka, S.; Hagel, J.; Schweitzer, D.; Strunz, W. κ-(BEDT−TTF)$_2$Cu[N(CN)$_2$]Br: A Fully Gapped Strong-Coupling Superconductor. *Phys. Rev. Lett.* **2000**, *84*, 6098–6101. [CrossRef]
30. Andraka, B.; Jee, S.C.; Kim, S.J.; Stewart, R.G.; Calson, D.K.; Wang, H.H.; Crouch SV, A.; Kini, M.A.; Williams, M.J. Specific heat of the high Tc organic superconductor κ-(ET)$_2$Cu[N(CN)$_2$]Br. *Solid State Commun.* **1991**, *79*, 57–59. [CrossRef]
31. Taylor, J.O.; Carrington, A.; Schlueter, A.J. Specific-Heat Measurements of the Gap Structure of the Organic Superconductors κ−(ET)$_2$Cu[N(CN)$_2$]Br and κ−(ET)$_2$Cu(NCS)$_2$. *Phys. Rev. Lett.* **2007**, *99*, 057001. [CrossRef]
32. Nakazawa, Y.; Kanoda, K. Low-temperature specific heat of κ-(BEDT-TTF)$_2$Cu[N(CN)$_2$]Br in the superconducting state. *Phys. Rev. B* **1997**, *55*, R8670–R8673. [CrossRef]
33. Sorai, M.; Nakazawa, Y.; Nakano, M.; Miyazaki, Y. Calorimetric Investigation of Phase Transitions Occurring in Molecule-Based Magnets. *Chem. Rev.* **2013**, *113*, 41–122. [CrossRef]
34. Souza, M.; Bartosch, L. Probing the Mott Physics in κ-(BEDT-TTF)$_2$X salts via thermal expansion. *J. Phys. Condens. Matt.* **2015**, *27*, 053203. [CrossRef]
35. Fournier, D.; Poirier, M.; Truong, K.D. Competition between magnetism and superconductivity in the organic metal κ-[BEDT-TTF]$_2$Cu[N(CN)$_2$]Br. *Phys. Rev. B* **2007**, *76*, 054509. [CrossRef]
36. Simizu, T.; Yoshimoto, N.; Nakamura, M.; Yoshizawa, M. High-frequency ultrasonic measurements of κ-(BEDT-TTF)$_2$Cu(NCS)$_2$ by devised transducer. *Phys. B* **2000**, *281&282*, 896–898. [CrossRef]
37. Imajo, S.; Nomura, T.; Kohama, Y.; Kindo, K. Nematic response of the Fulde-Ferrell-Larkin-Ovchinnikov state. *arXiv* **2021**, arXiv:2110.12774.
38. Imajo, S.; Kindo, K. The FFLO State in the Dimer Mott Organic Superconductor κ-(BEDT-TTF)$_2$Cu[N(CN)$_2$]Br. *Crystals* **2021**, *11*, 1358. [CrossRef]
39. Croitoru, M.D.; Buzdin, A.I. In search of unambiguous evidence of the Fulde-Ferrell-Larkin-Ovchinnikov state in quasi-low dimensional superconductors. *Condens. Matter* **2017**, *2*, 30. [CrossRef]
40. Croitoru, M.D.; Buzdin, A.I. The Fulde-Ferrell-Larkin-Ovchinnikov state in layered d-wave superconductors: In-plane anisotropy and resonance effects in the angular dependence of the upper critical field. *J. Phys. Condens. Matter* **2013**, *25*, 125702. [CrossRef]
41. Nakazawa, Y.; Taniguchi, H.; Kawamoto, A.; Kanoda, K. Electronic specific heat at the boundary region of the metal-insulator transition in the two-dimensional electronic system of κ−(BEDT−TTF)$_2$Cu[N(CN)$_2$]Br. *Phys. Rev. B* **2000**, *61*, R16295–R16298. [CrossRef]
42. Kagawa, F.; Itou, T.; Miyagawa, K.; Kanoda, K. Magnetic-Field-Induced Mott Transition in a Quasi-Two-Dimensional Organic Conductor. *Phys. Rev. Lett.* **2004**, *93*, 127001. [CrossRef]
43. Nakazawa, Y.; Kanoda, K. Thermodynamic investigation of the electronic states of deuterated κ−(BEDT−TTF)$_2$Cu[N(CN)$_2$]Br. *Phys. Rev. B* **1999**, *60*, 4263–4266. [CrossRef]
44. Nam, M.-S.; Mézière, C.; Batail, P.; Zorina, L.; Simonov, S.; Ardavan, A. Superconducting fluctuations in organic molecular metals enhanced by Mott criticality. *Sci. Rep.* **2013**, *3*, 3390. [CrossRef]
45. Powell, J.B.; McKenzie, H. Strong electronic correlations in superconducting organic charge transfer salts. *J. Phys. Condens. Matt.* **2006**, *18*, R827–R866. [CrossRef]
46. Kotliar, G.; Lange, E.; Rozenberg, M.J. Laudau Theory of the Finite Temperature Mott Transition. *Phys. Rev. Lett.* **2000**, *84*, 5180–5183. [CrossRef] [PubMed]
47. McWhan, B.D.; Remeika, P.J.; Rice, M.T.; Brinkman, F.M.; Maita, P.J.; Menth, A. Electronic Specific Heat of Metallic Ti-Doped V_2O_3. *Phys. Rev. Lett.* **1971**, *27*, 941. [CrossRef]
48. Malone, L.; Taylor, O.J.; Schlueter, A.J.; Carrington, A. Location of gap nodes in the organic superconductors κ-(ET)$_2$Cu(NCS)$_2$ and κ-(ET)$_2$Cu[N(CN)$_2$]Br determined by magnetocalorimetry. *Phys. Rev. B* **2010**, *82*, 014522. [CrossRef]
49. Kuroki, K.; Kimura, T.; Arita, R.; Tanaka, Y.; Matsuda, Y. d_{x2-y2}- versus d_{xy}- like pairings in organic superconductors κ−(BEDT−TTF)$_2$X. *Phys. Rev. B* **2002**, *65*, 100516. [CrossRef]
50. Kuroki, K. Pairing symmetry competition in organic superconductors. *J. Phys. Soc. Jpn.* **2006**, *75*, 051013. [CrossRef]

51. Guterding, D.; Altmeyer, M.; Jeschke, H.O.; Valentí, R. Near-degeneracy of extended s+d_{x2-y2} and d_{xy} order parameters in quasi-two-dimensional organic superconductors. *Phys. Rev. B* **2016**, *94*, 024515. [CrossRef]
52. Watanabe, H.; Seo, H.; Yunoki, S. Mechanism of superconductivity and electron-hole doping asymmetry in κ-type molecular conductors. *Nat. Commun.* **2019**, *10*, 3167. [CrossRef] [PubMed]
53. Milbradt, S.; Bardin, A.A.; Truncik, C.J.S.; Huttema, W.A.; Jacko, A.C.; Burn, P.L.; Lo, S.-C.; Powell, B.J.; Broun, D.M. In-plane superfluid density and microwave conductivity of the organic superconductor κ-$(BEDT\text{-}TTF)_2Cu[N(CN)_2]Br$: Evidence for *d*-wave pairing and resilient quasiparticles. *Phys. Rev. B* **2013**, *88*, 064501. [CrossRef]